



HAL
open science

General Statistics-Based Methodology for the Determination of the Geometrical and Mechanical Representative Elementary Volumes of Fractured Media

Ana Carolina Loyola, Jean-Michel Pereira, Manoel Porfírio P Cordão Neto

► **To cite this version:**

Ana Carolina Loyola, Jean-Michel Pereira, Manoel Porfírio P Cordão Neto. General Statistics-Based Methodology for the Determination of the Geometrical and Mechanical Representative Elementary Volumes of Fractured Media. Rock Mechanics and Rock Engineering, 2021, 10.1007/s00603-021-02374-6 . hal-03169749

HAL Id: hal-03169749

<https://enpc.hal.science/hal-03169749>

Submitted on 15 Mar 2021

HAL is a multi-disciplinary open access archive for the deposit and dissemination of scientific research documents, whether they are published or not. The documents may come from teaching and research institutions in France or abroad, or from public or private research centers.

L'archive ouverte pluridisciplinaire **HAL**, est destinée au dépôt et à la diffusion de documents scientifiques de niveau recherche, publiés ou non, émanant des établissements d'enseignement et de recherche français ou étrangers, des laboratoires publics ou privés.

General statistics-based methodology for the determination of the geometrical and mechanical Representative Elementary Volumes of fractured media

Ana Carolina Loyola · Jean-Michel Pereira ·
Manoel Porfírio Cordão Neto

Received: date / Accepted: date

Abstract The upscaling of mechanical properties of fractured media requires the definition of an appropriate size for the Representative Elementary Volume (REV). Because of the stochastic nature of the fracture networks, the REV size is not deterministic and should be defined based on the variability of the equivalent properties. This work presents a new general methodology to define the size of the REV for the geometrical and elastic moduli of fractured media. Following previous works on heterogeneous materials, the decision criterion is based on the precision error that arises from the statistical theory of samples. The proposed methodology also relies on the use of the Central Limit Theorem (CLT) to assess the REV of fractured rocks. The CLT is shown to theoretically apply to both the geometrical and the elastic equivalent properties. From that observation, a general equation is drawn to predict the variance of an equivalent property for any REV candidate size, provided that the variance for one size only is known. These concepts are tested using numerous finite element simulations to obtain the distribution of the equivalent elastic moduli of two-dimensional samples containing two fracture networks previously studied for their elastic properties. These properties are confirmed to tend to a normal distribution, as stated by the CLT. Also, the standard deviations associated to the tested REV sizes were predicted with accuracy from the standard

A. C. Loyola
Departamento de Engenharia Civil e Ambiental, FT – Universidade de Brasília, Brasília,
DF, Brasil
Navier, Ecole des Ponts, Univ Gustave Eiffel, CNRS, Marne-la-Vallée, France
E-mail: analoyolacr@gmail.com

J-M. Pereira
Navier, Ecole des Ponts, Univ Gustave Eiffel, CNRS, Marne-la-Vallée, France

M.P. Cordão Neto
Departamento de Engenharia Civil e Ambiental, FT – Universidade de Brasília, Brasília,
DF, Brasil

deviation obtained in the numerical simulations of only one proper reference volume. The mechanical REV was compared with the geometrical REV, which is based on the first invariant of the fracture tensor. Also, in order to reduce computational costs, a procedure to reduce the number of simulations of the reference volume was proposed. A preliminary verification of the applicability of the methodology to non-elastic problems was made. Proper predictions were obtained for the standard deviation of the compression strength calculated in two studies that considered, altogether, both two-dimensional and three-dimensional samples, as well as plastic and damage models.

1 Introduction

The influence of natural fractures was considered in well-known empirical (Hoek and Brown, 1997; Barton, 2002) and analytical (Duncan and Goodman, 1968; Oda et al., 1984) mechanical models for rock masses. Although these methods remain relevant, it was the incorporation of Discrete Fracture Networks (DFN) to numerical simulations that allowed a physically meaningful understanding of the role of complex fracture geometries in the hydro-mechanical behavior of geomaterials.

The explicit representation of all the fractures in a geological formation is hardly efficient or even impractical in the case of large numerical problems. For that reason, upscaling techniques emerged as a popular solution for incorporating the effects of the discontinuities while not compromising computational efficiency. These techniques consist in performing numerical experiments on samples of fractured rock masses and deriving equivalent properties to be used in large-scale simulations. One of the objectives of this type of study is to determine a proper Representative Elementary Volume (REV), that is, a sample size that allows the rock mass to be treated as a homogeneous medium. Since both the geometrical and hydro-mechanical properties of a rock mass suffer size effects, the task of defining the REV ultimately means to determine the dimensions for which these effects vanish.

Several studies have performed numerical mechanical experiments on fractured rock masses by incorporating DFNs in finite element models (Pouya and Ghoreychi, 2001; Yang et al., 2014; JianPing et al., 2015) and discrete methods (Min and Jing, 2003; Harthong et al., 2012; Rasmussen et al., 2018). When it comes to defining the size of the REV, a common methodology is to generate one DFN from the statistical characterization of field data and define the size for which the equivalent mechanical properties become stable. This approach disregards the non-unicity of the fracture networks and thus leads to the misconception that the results are deterministic, while they are statistical variables.

In fact, since uncertainty is inherent to fracture networks, the equivalent properties do not completely stabilize, but their standard deviation decreases as the REV size increases. Thus, a more rational approach is to define the REV based on an acceptable variability. Some works (e.g. Min and Jing, 2003;

Esmaili et al., 2010; Farahmand et al., 2018) used this concept to define a mechanical REV based on a maximum coefficient of variation. However, they did not perform enough realizations to observe the statistical distributions of the parameters and their conclusions apply only to the analyzed fractured rock masses.

As a consequence, studies on the REV of fractured rock masses still lack mathematical rigour and generality. The existent general recommendations for the definition of the REV usually relate its size to the joint trace length (Oda, 1988) or to joint spacing (Schultz, 1996) and differ between themselves, since they are drawn from the analysis of one specific rock mass.

Meanwhile, in the field of random composites, Kanit et al. (2003) used concepts from statistics to propose a general methodology for the determination of the REV. Their approach requires several numerical simulations to define the variance of an equivalent property as a function of volume; then, a relative error, based on the statistical theory of samples, is used as the criterion to define the REV size.

The present work brings these concepts to the context of the geometrical and the equivalent elastic properties of fractured rocks. We also propose here a statistics-based methodology to define the REV size using the precision error in Kanit et al. (2003); but by taking advantage of the Central Limit Theorem (CLT), this new approach requires simulations of only one REV size, and thus presents significant improvements in terms of efficiency.

The methodology here presented uses the crack tensor proposed by Oda (1982) and modified by Zhang and Einstein (2000) as an overall geometrical measure of the fracture networks. The crack tensor is a powerful tool to introduce generality to this approach; firstly, because it contains the combined effects of fracture length, orientation and intensity; secondly, because its elements follow the Central Limit Theory, and thus they tend to a normal distribution regardless of the statistical distributions of the fracture sets; and finally because its first invariant is known to be strongly related to the equivalent elastic properties (Kulatilake et al., 1993) and the equivalent strength (Kulatilake et al., 2001) of fractured rock masses.

Based on the applicability of the CLT, we propose a general equation to predict the standard deviation of a property for any REV size from the simulations of one size only. This equation, along with the other key concepts that base the methodology, is validated by generating a large number of fractured samples for two different DFNs and obtaining their equivalent elastic moduli. Also, preliminary tests that use published data on the equivalent uniaxial compression strength indicate that the methodology may also be extendable to non-elastic rock masses.

2 Theoretical background

We recall here two basic concepts that are useful to generalize the determination of the REV for the geometrical and elastic properties of fractured media.

The first one, which is the Central Limit Theorem, allows the assumption of normality of the geometrical properties of a DFN, no matter what the distributions of their features are. The second one, which is the crack tensor, is a robust measure of geometry known to be directly related to the equivalent mechanical properties.

2.1 Central Limit Theorem

Consider a variable X that follows a statistical distribution $f(X)$ with mean μ_X and standard deviation σ_X . By repeatedly taking a random sample of size n containing the elements X_1, X_2, \dots, X_n , it is possible to obtain a distribution $f(S_X)$ for a sum S_X of the form :

$$S_X = \frac{1}{T} \sum_{i=1}^n X_i \quad (1)$$

where T is an arbitrary scaling parameter.

The classical Central Limit Theorem (CLT), which is the second fundamental theorem of statistics, states that as $n \rightarrow \infty$ the distribution $f(S_X)$ approaches a normal distribution with mean μ_{S_X} and standard deviation σ_{S_X} , where:

$$\mu_{S_X} = \frac{n}{T} \mu_X \quad (2)$$

$$\sigma_{S_X} = \frac{\sqrt{n}}{T} \sigma_X \quad (3)$$

When S_X is the mean \bar{X} of X , $T = n$, and:

$$\mu_{\bar{X}} = \mu_X \quad (4)$$

$$\sigma_{\bar{X}} = \frac{\sigma_X}{\sqrt{n}} \quad (5)$$

The theorem is expected to give sufficiently accurate predictions when most of the generated terms are independent and when important outliers are not present or are ignored.

As for the minimum sample size for the assumption of normality to be valid, a general rule of thumb states that n must be at least 30. However, this size actually depends on the variable's distribution $f(X)$: it can be higher or lower than 30 depending on how close $f(X)$ is to a normal distribution.

2.2 Fracture Tensor

Fracture sets are described by the definition of statistical distributions for features such as intensity, density, length, strike and dip. When combined

in rock masses, they can form complex networks whose individual features are hard to describe mathematically. Nonetheless, an overall measure of the fracture network's geometry can be obtained by the definition of a fracture tensor, as initially proposed by Kachanov (1980) and Oda (1982).

We refer here to the following equation for the tensor F_{ij} , proposed by Zhang and Einstein (2000), which discards the arbitrary nondimensionalization of the previous formulations:

$$F_{ij} = \frac{1}{V} \sum_{k=1}^{n_f} S^{(k)} n_i^{(k)} n_j^{(k)} \quad (6)$$

where V is the volume of the rock mass, $S^{(k)}$ is the area of the k th discontinuity, and $n_i^{(k)}$ and $n_j^{(k)}$ are the components of the normal vector of the k th discontinuity with respect to the directions $i, j = x, y, z$. When working with two dimensions, Eq. (6) can be reformulated as:

$$F_{ij} = \frac{1}{A} \sum_{k=1}^{n_f} L^{(k)} n_i^{(k)} n_j^{(k)} \quad (7)$$

where A is the section area of the rock mass, $L^{(k)}$ is the length of the k th discontinuity and $i, j = x, y$. In these formulations, the first invariant of F_{ij} corresponds to the fracture intensity and thus has a clear physical meaning. In the two-dimensional case this first invariant I_1 is the areal intensity P_{21} , that is, the total length of fracture traces per area:

$$P_{21} = I_1 = F_{xx} + F_{yy} = \frac{1}{A} \sum_{k=1}^{n_f} L^{(k)} \quad (8)$$

By performing numerical compression tests on 3D samples of rock masses containing different fracture sets, Kulatilake et al. (1993) showed a strong relationship between the fracture tensor's first invariant and the equivalent elastic properties. Also, numerical and laboratory tests on artificial fractured samples performed by Kulatilake et al. (2001) showed that there is correlation between the peak strength and the fracture tensor diagonal components.

2.3 Defining a mechanical REV for Fractured Media

2.3.1 Generalities

The modelling of materials containing small, but relevant heterogeneities is frequently used to assess the role of the micro-structure on their behavior and to infer an equivalent constitutive model for large-scale simulations (e.g. Farahmand et al., 2018; Wang and Cai, 2020). In such cases, a proper scale of study must be set by the definition of a REV.

A REV is a domain usually required to follow three criteria: it must be representative of the geometrical pattern of the heterogeneities; it must be

large enough for the equivalent properties not to suffer from size effects; and its dimensions must be much smaller than those of the problem, so the principle of separation of scales is respected and the equivalent properties are valid to be applied in continuum mechanics.

In the field of rock mechanics, a distinction is usually made between the geometrical and the mechanical REV. The former can be determined by assessing size effects on quantities such as orientation, trace length and density, which may all be analyzed separately (e.g. Zhang et al., 2011), or in the overall measure of the fracture tensor (e.g. Wu and Kulatilake, 2012). As for the mechanical REV, it is commonly determined with numerical experiments (e.g. Pouya and Ghoreychi, 2001; Min and Jing, 2003; Esmaili et al., 2010; Jian-Ping et al., 2015; Ni et al., 2017). Although the two REV's are undoubtedly related, the sensitivity of the mechanical properties to size can be influenced by other factors than geometry, such as the materials parameters and the boundary conditions.

Early numerical studies on the REV of fractured rock masses test only one fracture network, overlooking the fact that the REV is not deterministic. Some recent works, however, accounted for the uncertain geometries of the samples and generated multiple DFNs to define the REV based on an acceptable coefficient of variation (COV) of the elastic properties. For instance, Esmaili et al. (2010) and Min and Jing (2003) performed 5 and 10 realizations, respectively, for each tested volume to obtain a relationship between size and variability.

Similarly, Kanit et al. (2003) acknowledged the non-uniqueness of the REV and proposed a statistic-based methodology to define the REV size for the elastic moduli and thermal conductivity of random composites. Their approach requires a number of simulations for each of the tested dimensions to obtain the variance of the properties as a function of size. Then, the theory of samples is used to calculate the volume associated to a user-defined relative error and degree of confidence; alternatively, one can impose a size and calculate the number of simulations necessary to attend such requirements. Their work deals with the inherent uncertainty of the REV with mathematical rigour and points out the subjective nature of the decision on its size, since an acceptable error must be selected and one can choose between performing few simulations of a large REV or many simulations of a smaller one.

The methodology proposed by Kanit et al. can be readily applied in fractured media studies, as was done by Caspari et al. (2016) for the calculation of dynamic elastic moduli of rocks containing horizontal fractures. However, performing several simulations for different domain sizes can become cumbersome when dealing with complex DFNs or non-linear problems, where the number of degrees of freedom and solving steps can be large; this is especially true when the chosen method requires large computation times.

We present hereafter how concepts of statistics apply to the definition of REV sizes for the elastic properties of fracture media. Following Kanit et al. (2003), we define a REV for the elastic properties that is based on a specified interval of confidence, but we reduce significantly the number of numerical simulations by introducing the CLT to this methodology.

2.3.2 A statistical point of view

The proper field sampling of a geological formation allows its fractures to be grouped in sets, according to the nature and the history of the discontinuities. The definition of a geometrical REV depends on the fracture network formed by the combination of the different sets in a rock mass, whose total number of fractures n_f in a given volume can be estimated as:

$$n_f = V \sum_{s=1}^{n_s} P_{30}^{(s)} = VP_{30} \quad (9)$$

where n_s is the number of sets, $P_{30}^{(s)}$ is the expected fractured density of the s th set and P_{30} is the expected fracture density of the network.

The distributions of the lengths and orientations of the fractures in a network are combinations of the distributions observed for its different sets and can take complex forms that may not be described by any known distribution function. Nonetheless, no matter what these distributions are, the CLT states that, taking a sufficient number of samples, any sum of the characterization variables follows a normal distribution.

All of the components in the fracture tensor, including its first invariant, are a sum S_f of the form:

$$S_f = F_{ij} = \sum_{k=1}^{n_f} \frac{Y^{(k)}}{V} \quad (10)$$

where $Y^{(k)}$ is a variable obtained from the product of geometrical features of the fracture k such as the normal vector components and area (see Equations (6) - (8)), and V is the volume of the rock mass, which can be replaced by (9) to obtain:

$$S_f = F_{ij} = \sum_{k=1}^{n_f} \frac{Y^{(k)} P_{30}^{(V)}}{n_f} = \sum_{k=1}^{n_f} \frac{X^{(k)}}{n_f} \quad (11)$$

Thus, each component of the fracture tensor is the average of a variable X that contains information on the geometry of a fracture and on the density over the domain. As such, regardless of what the distribution of Y is, the fracture tensor components tend to a normal distribution, as stated by the CLT, and their mean value and standard deviation can be estimated by Equations (4) and (5), where the sample size n is equal to the number of fractures n_f .

Considering two fractured REV's of volumes V_1 and V_2 and a parameter Z that follows a normal distribution, equation (5) can be used to establish the following relation:

$$\sigma_Z(V_2) = \sigma_Z(V_1) \sqrt{\frac{n_f(V_1)}{n_f(V_2)}} \quad (12)$$

where $\sigma_Z(V_1)$ and $\sigma_Z(V_2)$ are the standard deviations of Z for the volumes V_1 and V_2 and $n_f(V_1)$ and $n_f(V_2)$ are the average number of fractures in volumes V_1 and V_2 . By replacing the number of fractures in volumes V_1 and V_2 for (9) and considering that their P_{30} is approximately the same, (12) can be reformulated as:

$$\sigma_Z(V_2) = \sigma_Z(V_1) \sqrt{\frac{V_1}{V_2}} \quad (13)$$

If the REVs have squared cross sections and unit thickness, as is the case in two-dimensional problems, (13) can be further simplified to:

$$\sigma_Z(V_2) = \sigma_Z(V_1) \frac{l_1}{l_2} \quad (14)$$

where l_1 and l_2 are the sizes of the cross sections of volumes V_1 and V_2 .

Equations (12) - (14) show that it is possible to estimate the standard deviation associated to any REV size by obtaining the distribution of Z for one reference volume (V_1) only, given that this reference volume contains a sample size large enough for Z to have an approximately normal distribution. As the CLT applies to the fractures tensor, these equations can be used to easily define a proper size for the geometrical REV.

As for the equivalent mechanical properties, their variance can also be estimated with Equations (12) - (14) if they follow an approximately normal distribution. The results in (Kulatilake et al., 1993) show that the equivalent elastic properties are a non-linear function of the first invariant of the fracture tensor I_1 , which is the fracture intensity. But within a short range of I_1 , this relation is roughly linear, as will be shown later; in this case, the elastic moduli will also follow an approximately normal distribution.

From the statistical theory of samples, a relative error ε_{rel} for the average \bar{Z} of the parameter Z can be defined based on its confidence interval as:

$$\varepsilon_{rel} = \frac{\varepsilon_{abs}}{\bar{Z}} = t^*_{n_Z-1, \alpha} \frac{\sigma_Z(V)}{\bar{Z}\sqrt{N}} \quad (15)$$

where N is the number of realizations of a REV of volume V used to estimate Z ; ε_{abs} is the absolute error; $t^*_{n_Z-1, \alpha}$ is the t-value for a significance level α and $n_Z - 1$ degrees of freedom; and n_Z is the number of samples of Z used to estimate \bar{Z} and σ_Z .

As in the methodology by Kanit et al. (2003), the precision error in (15) is suggested here as a decision parameter for the REV size. The REV can be defined as the volume for which one simulation ($N = 1$) is necessary to estimate the average property \bar{Z} with a certain relative error. If a volume V is selected based on 95% degree of confidence, for example, this means that a REV of volume V has a 95% chance of returning a value of \bar{Z} that lies within the range of $\bar{\mu}_Z \pm \varepsilon_{abs}$, where μ_Z is the true mean of Z . Alternatively, one can use Equation (15) to impose a volume and calculate the number of realizations N required to reach the error criterion for the average property.

3 Methods

The applicability and generality of the concepts presented above are assessed with numerical tests on the fracture networks studied by Yang et al. (2014) and Min and Jing (2003), which will be hereinafter referred to as Networks 1 and 2, respectively. Their statistical characterization is presented in Tables 1 and 2.

While Network 1 is constituted of two fractures sets with orientations, lengths and spacing described by normal distributions, Network 2 has four sets where the fractures length follows a fractal scaling law and their orientation follows a Fisher distribution. The resulting probability density function (pdf) of the fracture's length for both networks is presented in Figures 1 and 2. Note that the pdf for Network 1 is presented alongside a normal distribution with same mean and standard deviation, so their differences in skewness and kurtosis become clear.

Both Min and Jing (2003) and Yang et al. (2014) performed numerical simulations to obtain the homogenized elastic properties for different REV sizes. While Yang et al. (2014) generated one DFN to study size effects and anisotropy of the elastic compliance tensor by finite element modelling, Min and Jing (2003) used the distinct element method to determine the REV based on the COV of the elastic properties of 10 different DFNs.

A similar methodology was followed here; but with the purpose of obtaining a statistical distribution for the geometrical and elastic properties, 1000 DFNs were generated for each network. The finite element method was chosen to perform the simulations. The adopted procedure is the following:

[1] Generate discrete fracture networks For each case study, 1000 DFNs were originally generated in the largest domains to be tested. The centers of the fractures were generated with a Poisson process, and their lengths and orientations were generated according to the distributions given in Tables 1 and 2. In order to verify size effects, increasingly smaller domains were cut out from the original REV while maintaining the same geometrical center, as shown in Figure 3. At each size reduction, the fractures whose centers lied outside of the new domain were removed; those whose centers lied inside the new domain but intersected its boundaries had their lengths adjusted. The purpose of the removal of the external fractures is to not consider fractures that would not be generated by an independent Poisson process at each REV size. As a result, the average fracture density P_{30} was guaranteed to be approximately the same for the tested sizes and the simplified equation (14) could be used.

Network 1 was tested for 11 different squared REVs with sizes that ranged from 2 m x 2 m to 22 m x 22 m; Network 2 was tested for 9 sizes that ranged from 0.5 m x 0.5 m to 8 m x 8 m.

[2] Generate the mesh Finite element meshes constrained by the DFNs were generated with recursive calls to the open-source mesh generator Triangle (Shewchuk, 1996). To guarantee a good mesh quality, the triangular elements

were specified to have a minimum angle of 20 degrees and maximum area of 0.1 m^2 . Figures 4 and 5 show an example of a generated DFN and mesh for each study case. Table 3 presents the number of degrees of freedom in the generated meshes.

After generating the triangular mesh, the open source code ciGen (Nguyen, 2014) was called to generate zero-thickness interface elements (Goodman et al., 1968) to represent the discontinuities. The original ciGen code allows the creation of interface elements either in the frontiers between two materials or in all the elements boundaries. We extended the code to allow the creation of interface elements only at the frontiers where fractures are present.

Figure 6 illustrates the creation of the interface elements. The nodes where fractures are present are duplicated to create four-node zero-thickness elements. In general, no new node is created at the fractures ends, but the existing node is simply repeated in order to prevent displacement jumps when the discontinuity terminates. An exception occurs when the fracture terminates at the boundary of the domain, so the discontinuities at the boundaries can be properly represented. The fractures delimit zones for the elements that will determine their new connectivity. Figure 6 illustrates the changes in elements containing a node that: (a) is intercepted by one fracture, (b) is intercepted by several fractures and (c) is at the boundary of the domain.

[3] *Obtain equivalent elastic tensor* Both the intact rock and the fractures are considered to be linear elastic materials. Their properties are described in Table 4. The equivalent elastic compliance tensor for the fractured samples was obtained via homogenization. The three linearly independent stress boundary conditions in Figure 7 were applied sequentially and, from the resulting equivalent strains, the tensor was calculated. This procedure is well detailed by Yang et al. (2014) and Min and Jing (2003) and also recalled in Appendix A. In this work, we will focus on the equivalent elastic moduli E_x and E_y and the equivalent shear modulus G_{xy} , which are obtained from the diagonal terms of the tensor in Equation 13 of the Appendix A.

A finite element code was implemented to solve the plane strain problems. To validate the FEM analyses, the equivalent moduli for orthogonal sets of persistent and equally spaced fractures were obtained. A fracture spacing of 0.5 m and the elastic parameters of Network 1 were used. The comparison of these results with the analytical solution by Duncan and Goodman (1968) is presented in Figure 8.

For some of the generated fracture networks the finite element analysis returned invalid values due to mesh errors, mainly caused by the precision of the Triangle output files. Table 5 presents the tested sizes and the number of successful simulations for each of them.

4 Results

4.1 Distributions of the geometrical and elastic properties

Figures 9 and 10 show the Q-Q plot for I_1 and E_y and the normal Q-Q plot as a reference line. They exemplify how the distributions for both geometrical and elastic properties approach a normal distribution as the REV size increases.

Besides this visual inspection, the normality of the distributions can be assessed with their values of skewness and excess kurtosis, which are presented in Tables 6 and 7. The skewness is a measure of asymmetry and the excess kurtosis is a measure of shape, regarding the pick and the tails of a distribution, in comparison to a normal one. Since the skewness and excess kurtosis of a normal distribution are equal to zero, these data also show that larger REV sizes have distributions which are closer to a normal one. We use here the general rule of thumb of establishing maximum absolute values of 0.5 and 1.0 for the skewness and kurtosis, respectively, as a criterion to attest the normality of a distribution. This criterion is conservative when compared to the confidence intervals built by Jones (1969) for these parameters

Both Networks 1 and 2 presented considerably asymmetrical distributions for the smallest REVs. This is because their dimensions are not larger than the average fracture spacing, and thus some of the tested domains did not contain any fractures. For Network 1, the size of 6 m is shown to return fairly normal distributions. This size has, on average, 15 fractures. As for Network 2, approximate normal distributions are obtained for sizes larger than 2 m, which would have an expected number of fractures of at least 74. As Network 2 presents a length distribution that is further from normality than Network 1's one, it is unsurprising that it requires a larger sample size (74 fractures for Network 2 vs 15 for Network 1) to obtain an approximately normal distribution of the tested parameters.

The elastic properties were expected to follow a normal distribution if they were approximately linear functions of I_1 . Indeed, Figures 11 and 12 show that a linear equation is a good estimation for the relationship between these variables. The non-perfect fitting of the data can be explained by two main reasons. Firstly, a power function would be an even better fit for the relationship between elastic moduli and the first invariant of the fracture tensor, which agrees with the results in Kulatilake et al. (1993); secondly, the variability of the equivalent properties are influenced by other geometrical features than the fracture intensity, such as the particular intersections between the fractures in each DFN and their resulting meshes. Despite of these particularities, the strong correlations in Figures 11 and 12 suggest that fracture intensity is much more influential on the equivalent elastic properties.

As a result of the non-perfect adequacy of the linear fitting, it can be seen in Tables 6 and 7 that the data for the elastic moduli is slightly more skewed than those of I_1 . Nonetheless, their distributions can also be considered as approximately normal.

4.2 Inference of the standard deviations with the CLT

Figures 13 and 14 present the average, maximum and minimum values for I_1 and the elastic moduli. As stated by the CLT, the average values remain approximately the same while the properties vary in shorter ranges as the REV size increases.

In order to test the applicability of equation (14), a reference volume must be set to predict the standard deviations of the other sizes. For each network, the smallest sizes to produce approximately normal distributions and for which the average values stabilized were chosen; that is, the 6 m x 6 m domain for Network 1 and the 3 m x 3 m domain for Network 2. Figures 15 and 16 show the standard deviations for I_1 , E_x , E_y and G_{xy} obtained from the simulations of the REVs and from Equation (14), which uses the standard deviations of the reference volumes to predict the standard deviations of the other sizes.

There is a good agreement between the results, except for the smallest sizes, which have distributions that are very distant from normality. Thus, it is demonstrated that the simulation of many different sizes is unnecessary in the search for a REV for the geometrical and elastic properties of fractured media. Since the CLT applies to both geometrical and elastic properties, it is only necessary to simulate one suitable size, that is, a volume for which the properties have approximately normal distributions, and the variance associated to any other volume can be inferred.

Figure 17 compares the coefficient of variations for both the first invariant of the fracture tensor and the equivalent elastic moduli. Figure 17b also shows the COV calculated by Min and Jing (2003). The main sources of discrepancies are their smaller number of samples and their approach to generate the fractured sample, which removes isolated fractures and dead-ends. For both cases the COV of I_1 was larger than that of the elastic properties, which suggests that the geometrical REV is larger than the mechanical REV. It can be also observed that Network 2 shows considerable proximity between the COV of the first invariant and those of the elastic properties; this may be due to its high fracture intensity, which controls the variability of the elastic moduli. These results indicate that the geometrical REV can be used as a conservative estimation of the mechanical REV. This is, however, a controversial topic. While some studies also report that the geometrical REV is larger than the mechanical REV, others concluded the opposite (e.g. Esmaili et al., 2010; Ni et al., 2017). Hence, more investigations on the relationship between the variability of I_1 and the elastic properties would be required before a decisive conclusion can be drawn.

Table 8 presents the precision errors calculated with Equation (15) for each REV size using a degree of confidence of 95%. From these data, it can be concluded, for example, that a random 20 m x 20 m REV for Network 1 has a 95% chance of returning a value of E_y that differs from its true mean by 9.9% or less. Table 9 presents the number of realizations of different volume sizes required to reach relative errors of 5% and 1%. The best choice between performing fewer simulations of large volumes or more simulations of

smaller volumes depends on the method used to solve the linear systems and its computational complexity, in the case of the finite element method.

By setting an acceptable error of 10 %, the geometrical REV size for Networks 1 and 2 would be 34 m and 6 m, respectively. As for the mechanical REV size, it would be 18 m for Network 1 and 5 m for Network 2. Yang et al. (2014) select for Network 1 a REV size of 12 m, which is associated to a maximum error of 16.5 %. Min and Jing (2003) recommend an acceptable COV between 5% and 10%, which puts the REV size between 3 m and 6 m, according to their data.

Table 10 shows the REV size for four existing approaches and the precision error for the mechanical properties attributed to them. Three approaches that provide a ratio between factor size and geometrical features are compared: 3 times the average trace length, as suggested by Oda (1988); 10 times the average trace length and 10 times the average spacing, which were used by a number of authors as pointed out by Ni et al. (2017) and Liu et al. (2018). The fourth approach is the definition of the size based on a 10% acceptable COV, which is a common criterion in the studies that perform tests in more than one sample. The methodologies that apply a factor of 10 to the average spacing and length were shown to be conservative approaches. As for the fourth approach, since the precision error is the COV multiplied by the t-value (see Equation (15)), it is always bigger than the COV itself. For a 95% degree of confidence, the minimum t-value is 1.96, and so, considering the suggested error of 10 % and the theory of samples, a COV not bigger than 5% should be considered acceptable.

4.3 Number of simulations

The number of simulated REV's of the reference size should ideally be large, so the estimation of the standard deviation for the elastic moduli is accurate. As the sample variance of a normally distributed variable is known to follow a chi-squared distribution, a confidence interval for the standard deviation can be estimated. Table 11 presents the confidence interval for standard deviations (SD) of samples with different sizes, based on a 95% degree of confidence.

The number of approximately 1000 simulations used to obtain the moduli distribution makes it possible to attest, with 95% confidence, that the estimated sample standard deviations do not differ more than 5% of the true standard deviations. This number of simulations may be impracticable depending on the nature of the problem, but a smaller sample of REV's can be chosen based on the confidence intervals in Table 11. For example, if a maximum difference of 11% is judged to be acceptable, 200 simulations of the reference volume could be used to estimate the standard deviation of the parameters.

When the feasible number of simulations is very small, if the sample of tested REV's is completely random, the standard deviations of the parameters are probably going to be inaccurate. However, these inaccurate estimations can

be avoided by using the distribution of the geometrical properties to select an optimum small sample to be taken to the numerical analyses. Since the random generation of fractures is usually not computationally expensive, a large sample of DFNs is easily obtained and the standard deviation of the fracture tensor elements can be estimated with accuracy. A small optimized sample of REV's can be taken from the original one, by requiring it to have similar averages and standard deviations to those of the large sample. As the elastic moduli are directly related to the diagonal terms of the fracture tensor, a small sample that returns accurate statistical estimators for these terms should also provide good estimators for the elastic properties distributions.

This suggestion was tested for 50 and 10 simulations of the reference volumes of Networks 1 and 2. An algorithm was implemented to generate random combinations of 50 and 10 DFNs from the original sample, until the sample standard deviations and averages for each diagonal term of the fracture tensor (F_{xx} and F_{yy}) did not differ in more than 5% from those of the sample of 1.000 DFNs. The results for the homogenization of the selected samples in Table 12 show that the average and the standard deviations of the elastic moduli can be estimated from small samples, when those are carefully selected. Table 13 shows the calculated errors for the maximum tested volumes. Since more uncertainty is attributed to the smaller samples, they have a higher t-value and tend to have higher predicted errors and larger selected REV's. This is an advantage of the criterion based on the precision error, in comparison to criteria based on a maximum COV: it takes into account not only the standard deviation of the property, but also the uncertainty attributed to the sample size.

4.4 Applicability to non-elastic problems

The fracture network in a rock mass does not affect only its deformability, but also reduces its strength and changes its mechanisms of failure. Because of that, many works considered plastic models for the fractures in order to reproduce brittle failure and assess the upscaled strength of rock masses with numerical experiments (Kulatilake et al., 2001; Pouya and Ghoreychi, 2001; Esmaili et al., 2010; Harthong et al., 2012; Wang et al., 2013; JianPing et al., 2015; Farahmand et al., 2018; Rasmussen et al., 2018).

Most of the referred works contain size effects studies in order to obtain the dimensions of the REV. Also, some investigate the relation between upscaled strength and the geometry of the DFN. Kulatilake et al. (2001), Harthong et al. (2012) and Wu and Kulatilake (2012) showed that the rock strength is strongly related to the diagonal elements of the crack tensor. Their results indicate the possibility of applying the methodology here presented to obtain the REV for the rock mass strength. Like the elastic moduli, the rock mass strength was shown to have a non-linear relation with the fracture tensor within the large range of fracture intensities tested by the authors. Considering only the shorter range of intensity related to the variability of the geometrical

properties, however, this relation could be considered roughly linear and the CLT would apply to the rock strength too.

We test this hypothesis for the data in Esmaili et al. (2010) and Farahmand et al. (2018). These studies measured the Uniaxial Compressive Strength (UCS) of fractured rock masses for several samples of different sizes in order to estimate the size of the REV based on an acceptable COV. Both performed numerical experiments using DEM. Esmaili et al. (2010) used 3D samples and tested 5 REVs of each tested size; Farahmand et al. (2018) used 2D samples and performed from 3 to 10 REVs of each tested size; they also considered fracture propagation by the inclusion of a cohesive crack model. A summary of their data is presented in Tables 14 and 15.

We chose the reference volume to predict the standard deviations in Esmaili et al. (2010) using the average number of fractures for each REV size. The first REV to attend to the rule of thumb of 30 fractures is that with dimensions 1.5 m x 1.5 m x 3 m. As the number of samples is small and distributions are far from normal, we chose the immediately superior size of 3.5 m x 3.5 m x 7.0 m as a reference volume. Figure 18 shows the calculated standard deviations, their confidence interval based on a sample size of 5 and the predictions made with (12). The estimated standard deviations are all inside the confidence intervals and are close to those obtained by the DEM simulations.

Since Farahmand et al. (2018) do not provide the number of fractures in each sample, we used Equation (13) to estimate their results. Figure 19 shows that reasonable predictions of the standard deviation of I_1 can be made from the REV of dimensions 5 m x 2 m. Again, we chose the immediately larger REV of 7 m x 2.8 m to estimate the standard deviation of the UCS, as shown in Figure 20. Fair predictions were obtained for the volumes larger than the reference REV; for the 5 m x 2.0 m domain, the estimation is inside the interval of confidence, but distant from the value calculated from the simulations. Besides the small number of samples, this could be explained by a possible difference in the fracture densities of the REVs, which would make Equation (13) inappropriate. In fact, since this work considers fracture propagation, it is likely that distinct volumes have differences in their fracture density at failure. Anyhow, the results obtained for the sizes larger than 7 m x 2.8 m are encouraging and tend to show that the methodology here presented can be extended to non-elastic parameters.

5 Proposed Methodology

A proper REV size for the mechanical and geometrical parameters of fractured media can be defined based on the accepted variability of a property, which is here measured by the precision error associated to its confidence interval. Only one reference volume must be simulated in order to obtain statistical estimators for the elastic properties of any other REV size. From the theoretical concepts and the results presented in this work, the following methodology for

the definition of the geometrical and mechanical REV size of elastic fractured media is proposed:

[1] *Choose a reference volume* Select a reference volume that returns approximate normal distributions for the properties. An initial guess for the reference volume can be made by using the rule of thumb that defines a minimum sample size of 30; thus, a volume for which there are at least 30 fractures can be used to generate a large sample of DFNs. An appropriate number of generated DFNs can be selected using Table 11. If the obtained distribution for the first invariant of the fracture tensor is approximately normal, the choice of the geometric reference volume is valid. Since the data for the elastic moduli tends to be more skewed than the first invariant of the fracture tensor, we recommend the reference volume of the mechanical tests to be larger than the geometrical reference volume, specially if the number of REVs to be tested is small.

[2] *Obtain homogenized properties* Perform numerical tests on the REVs to obtain the elastic moduli and their statistical distributions for the reference size. If it is not viable to simulate all the generated DFNs, a smaller sample can be selected for the numerical problem. A small sample which returns similar statistical estimators for the diagonal terms of the fracture tensor than a large sample is more likely to return appropriate estimators for the elastic parameters. In this work, a maximum difference of 5% in the averages and standard deviations was used to select small samples.

[3] *Predict standard deviations for other sizes* Use Equation (12) or Equation (13) (if the fracture density does not vary significantly between REV sizes) to calculate the standard deviations of the elastic moduli for any other REV size. Use Equation (15) to obtain the predicted errors.

[4] *Select REV size* Set a maximum precision error and select the volume of work and the number of simulations N that will be used to estimate the average properties.

Although the upscaling of the elastic moduli performed here use 2D samples, the methodology can be readily applied in 3D cases since the fracture tensor is formulated for three dimensions and the same relationship between I_1 and the elastic moduli holds for 3D samples, as shown by Kulatilake et al. (1993).

6 Conclusions

The generation of DFN models is a stochastic process. Since the location, the intensity and the geometrical features of the fractures are random variables, an infinite number of fracture networks can be generated from the distributions that describe the field data. Thus, any equivalent property of fractured masses

has an intrinsic variability, which can be used as a criterion to define a proper representative volume.

Following this idea, we presented here how the statistical theory of samples apply to the definition of a representative volume for fractured media. The fracture tensor was used as an overall measure of geometry and its elements were shown to theoretically follow a normal distribution, regardless of the distributions of the fractures features. The assumption of normality was also shown to be extendable to the elastic properties, assuming that the fracture intensity does not vary within very big ranges. Based on the normality of the geometrical and elastic properties, their standard deviations were shown to be predictable with a general equation for any REV size, provided that the standard deviation for one volume is known.

These concepts were tested for two different discrete networks previously studied for their elastic properties. The results showed that the distribution of the first invariant of the fracture tensor and of the elastic properties indeed tend to be a normal distribution. Also, the standard deviations of different REV sizes were predicted with accuracy from the simulations of one reference volume. Finally, it was shown that performing a large number of simulations can be avoided by selecting an optimized small sample from the generated DFNs.

The procedure used to predict the standard deviations of the elastic moduli was included in a new general methodology for the determination of the REV for the geometrical and the elastic properties. We adopt the precision error associated to the confidence interval of the average properties as the decision parameter, as was made in previous REV studies.

Based on a precision error of 10%, we selected sizes for the geometrical and the mechanical REVs. For both study cases the geometrical REV is larger, and this difference is more significant for Network 1, which has a considerably lower fracture intensity. The comparison between geometrical and mechanical REVs led to variate conclusions in previous studies, so further investigation is needed before attesting that the geometrical REV size is always a conservative estimation for the mechanical REV. The approach presented here was also compared against some empirical, purely geometrical rules and the COV-based criterion. Some of the geometry-based rules were shown to be conservative for the studied networks, which indicates that they may be safe estimations. As for the COV, it is directly related to the precision error used in this work, but the latter has the advantage of accounting for the number of tested samples.

Since the rock mass equivalent strength is sometimes also required in the upscaling of mechanical properties, we verified the application potential of the methodology to non-elastic problems using available data on the UCS of fractured samples. Considering the small numbers of samples and their associated interval of confidence, we obtained fair predictions for the standard deviations of the UCS. These results indicate that the methodology may be applicable to non-elastic materials. There is also a solid theoretical background to support this idea since, like the elastic moduli, the rock strength is strongly related to the fracture tensor. Nonetheless, the small amount of data only

allows this verification to be considered preliminary. More rigorous statistical studies on the compression strength and other plasticity-related properties need to be conducted in order to attest the applicability of the methodology and to investigate the eventual need for adaptations to non-elastic problems.

In this work, the fracture tensor was chosen as a measure of geometry because it incorporates several geometrical features. It can be used for two-dimensional and three-dimensional samples and it has proved relationship with the equivalent mechanical properties of rock masses. However, the CLT applies to any other average or sum of the geometrical features that may be preferred to quantify geometry.

At last, in order to successfully apply the proposed methodology, it is important to set a proper scale of study and to guarantee that no important outliers are present in the fracture network, so that the CLT is valid.

Appendices

A Calculation of the equivalent elastic properties

The stress-strain relationship for linear elastic anisotropic media can be expressed as:

$$\varepsilon_{ij} = S_{ijkl}\sigma_{kl} \quad (16)$$

We consider here the equivalent compliance tensor of a fractured rock mass where the intact rock has Young modulus E_r and Poisson ratio ν_r . In the two-dimensional space, the constitutive tensor S_{ijkl} can be expressed in terms of the equivalent elastic moduli as:

$$S_{ijkl} = \begin{bmatrix} S_{11} & S_{12} & S_{13} & S_{14} \\ S_{21} & S_{22} & S_{23} & S_{24} \\ S_{31} & S_{32} & S_{33} & S_{34} \\ S_{41} & S_{42} & S_{43} & S_{44} \end{bmatrix} = \begin{bmatrix} \frac{1}{E_x} & -\frac{\nu_{yx}}{E_y} & -\frac{\nu_{zx}}{E_z} & \frac{\eta_{x,xy}}{G_{xy}} \\ -\frac{\nu_{xy}}{E_x} & \frac{1}{E_y} & -\frac{\nu_{zy}}{E_z} & \frac{\eta_{y,xy}}{G_{xy}} \\ -\frac{\nu_{xz}}{E_x} & -\frac{\nu_{yz}}{E_y} & \frac{1}{E_z} & \frac{\eta_{z,xy}}{G_{xy}} \\ \frac{\eta_{xy,x}}{E_x} & \frac{\eta_{xy,y}}{E_y} & \frac{\eta_{xy,z}}{E_z} & \frac{1}{G_{xy}} \end{bmatrix} \quad (17)$$

where E_i are the elastic moduli, ν_{ij} are Poisson ratios, $\eta_{i,jk}$ are coefficients of mutual influence of the first kind and $\eta_{ij,k}$ are coefficients of mutual influence of the second kind. Considering that the fractures have strikes in the direction z , they do not affect the deformations in this direction; thus, $E_z = E_r$, $\nu_{xz} = \nu_{yz} = \nu_r$, and the components S_{31} , S_{32} and S_{33} are then equal to those of the compliance tensor of the intact rock. Also, since the shear stress σ_{xy} does not affect deformations in z , S_{34} is equal to zero. Considering the symmetry conditions, $S_{13} = S_{31}$, $S_{23} = S_{32}$ and $S_{34} = S_{43}$. Hence, there are 7 components of the tensor which are known a priori because of the assumption of bidimensionality.

For plane-strain conditions, the relationship in (16) reduces to:

$$\begin{bmatrix} \varepsilon_x \\ \varepsilon_y \\ 0 \\ \gamma_{xy} \end{bmatrix} = \begin{bmatrix} S_{11} & S_{12} & S_{13}^r & S_{14} \\ S_{21} & S_{22} & S_{23}^r & S_{24} \\ S_{31}^r & S_{32}^r & S_{33}^r & 0 \\ S_{41} & S_{42} & 0 & S_{44} \end{bmatrix} \begin{bmatrix} \sigma_x \\ \sigma_y \\ \sigma_z \\ \tau_{xy} \end{bmatrix} \quad (18)$$

Three linearly-independent boundary conditions are necessary to obtain the unknowns of the elastic compliance tensor. In this paper, we used the applied stresses illustrated in Figure 7. The resulting displacements u_i ($i = x, y$) at the boundaries were used to calculate the homogenized strains as:

$$\varepsilon_{ij} = \frac{u_{i,j} + u_{j,i}}{2} \quad (19)$$

The stress σ_z can be calculated from the applied stresses and the properties of the intact rock as:

$$\sigma_z = -\frac{S_{31}^r \sigma_x + S_{32}^r \sigma_y}{S_{33}^r} \quad (20)$$

And the tensor components are calculated using (20) and the system formed by lines 1, 2 and 4 in (18)

References

- Barton N (2002) Some new Q-value correlations to assist in site characterisation and tunnel design 39:185–216
- Caspari E, Milani M, Rubino J, Müller T, Quintal B, Holliger K (2016) Numerical upscaling of frequency-dependent p- and s-wave moduli in fractured porous media. *Geophysical Prospecting* 64:1166–1179
- Duncan JM, Goodman RE (1968) Finite element analyses of slopes in jointed rock: A report of an investigation. Tech. Rep. S-68-3, U.S. Army Corps of Engineers
- Esmaili K, Hadjigeorgiou J, Grenon M (2010) Estimating geometrical and mechanical REV based on synthetic rock mass models at Brunswick Mine. *International Journal of Rock Mechanics and Mining Sciences* 47:915–926
- Farahmand K, Vazaios I, Diederichs MS, Vlachopoulos N (2018) Investigating the scale-dependency of the geometrical and mechanical properties of a moderately jointed rock using a synthetic rock mass (SRM) approach. *Computers and Geotechnics* 95:162–179
- Goodman R, Taylor R, Brekke T (1968) A model for the mechanics of jointed rock. *Journal of the Soil Mechanics and Foundations Division* 94
- Harthong B, Scholtès L, Donzé FV (2012) Strength characterization of rock masses using a coupled DEM-DFN model. *Geophysical Journal International* 191(2):467–480
- Hoek E, Brown ET (1997) Practical estimates of rock mass strength. *International Journal of Rock Mechanics and Mining Sciences* 34(8):1165–1186

- JianPing Y, WeiZhong C, DianSen Y, JingQiang Y (2015) Numerical determination of strength and deformability of fractured rock mass by FEM modeling. *Computers and Geotechnics* 64:20–31
- Jones TA (1969) Skewness and kurtosis as criteria of normality in observed frequency distributions. *Journal of Sedimentary Research* 39(4):1622–1627
- Kachanov M (1980) Continuum model of medium with cracks. *J Engng Mech Div, ASCE* 106:1039–1051
- Kanit T, Forest S, Galliet I, Mounoury V, Jeulin D (2003) Determination of the size of the representative volume element for random composites: statistical and numerical approach. *International Journal of Solids and Structures* 40:3647–3679
- Kulatilake PHSW, Wang S, Stephansson O (1993) Effect of finite size joints on the deformability of jointed rock in three dimensions. *Int J Rock Mech Min Sci & Geomech* 30:479–501
- Kulatilake PHSW, Malama B, Wang J (2001) Physical and particle flow modeling of jointed rock block behavior under uniaxial loading. *International Journal of Rock Mechanics & Mining Sciences* 38:641–657
- Liu Y, Wang Q, Chen J, Song S J Zhan, Han X (2018) Determination of geometrical revs based on volumetric fracture intensity and statistical tests. *Appl Sci* 8(800):1–18
- Min K, Jing L (2003) Numerical determination of the equivalent elastic compliance tensor for fractured rock masses using the distinct element method. *International Journal of Rock Mechanics and Mining Sciences* 40:795–816
- Nguyen VP (2014) An open source program to generate zero-thickness cohesive interface elements. *Advances in Engineering Software* 74:27–39
- Ni P, Wang S, Wang C, Zhang S (2017) Estimation of the REV size for fractured rock mass based on damage coefficient. *Rock Mechanics and Rock Engineering* 50:555–570
- Oda M (1982) Fabric tensor for discontinuous geological materials. *Soils and Foundations* 22:96–108
- Oda M (1988) A new method for evaluating the representative elementary volume based on joint survey of rock masses. *Can Geotech J* 25:440–447
- Oda M, Suzuki K, Maeshibu T (1984) Elastic compliance for rock-like materials with random cracks 24:27–40
- Pouya A, Ghoreychi M (2001) Determination of rock mass strength properties by homogenization. *International Journal for Numerical and Analytical Methods in Geomechanics* 25(13):1285–1303
- Rasmussen LL, de Farias MM, de Assis AP (2018) Extended Rigid Body Spring Network method for the simulation of brittle rocks. *Computers and Geotechnics* 99:31–41
- Schultz R (1996) Relative scale and the strength and deformability of rock masses. *Journal of Structural Geology* 18(9):1139–1149
- Shewchuk JR (1996) Triangle: Engineering a 2D Quality Mesh Generator and Delaunay Triangulator. In: *Applied Computational Geometry: Towards Geometric Engineering*, Lecture Notes in Computer Science, vol 1148, Springer-Verlag, pp 203–222, from the First ACM Workshop on Applied Computa-

tional Geometry

- Wang S, Huang R, Ni R P, Gamage, Zhang M (2013) Fracture behavior of intact rock using acoustic emission: experimental observation and realistic modeling. *Geotechnical Testing Journal* 36(6):903–914
- Wang X, Cai M (2020) A DFN–DEM Multi-scale Modeling Approach for Simulating Tunnel Excavation Response in Jointed Rock Masses. *Rock Mechanics and Rock Engineering* 53(3):1053–1077, URL <https://doi.org/10.1007/s00603-019-01957-8>
- Wu Q, Kulatilake PHSW (2012) REV and its properties on fracture system and mechanical properties, and an orthotropic constitutive model for a jointed rock mass in a dam site in china. *Computer and Geotechnics* 43:124–142
- Yang J, Chen W, Y D, Yu H (2014) Numerical determination of elastic compliance tensor of fractured rock masses by finite element modeling. *International Journal of Rock Mechanics and Mining Sciences* 70:474–482
- Zhang L, Einstein H (2000) Estimating the intensity of rock discontinuities. *International Journal of Rock Mechanics and Mining Sciences* 37:819–837
- Zhang W, Chen JP, Liu C, Huang R, Li M, Zhang Y (2011) Determination of geometrical and structural representative volume elements at the Baihetan dam site. *Rock Mechanics and Rock Engineering* 45:409–419

Table 1 Statistical parameters for Network 1, from Yang et al. (2014)

	Dip orientation			Length			Density (1/m ²)
	Type	Mean	Stand. Dev.	Type	Mean (m)	Stand. Dev. (m)	
1	Normal	150	10.0	Normal	4	1	0.16
2	Normal	50	7.0	Normal	3	0.7	0.25

Table 2 Statistical parameters for Network 2, from Min and Jing (2003)

	Orientation			Length			Density (1/m ²)
	Type	Mean	k^*	Type	Mean (m)	D^*	
Set 1	Fisher	8/145	5.9	Fractal	0.92	2.2	4.6
Set 2	Fisher	88/148	9.0	Fractal	0.92	2.2	4.6
Set 3	Fisher	76/21	10.0	Fractal	0.92	2.2	4.6
Set 4	Fisher	69/87	10.0	Fractal	0.92	2.2	4.6

Table 3 Number of degrees of freedom in the finite element problems

Network 1											
Size (m)	22.0	20.0	18.0	16.0	14.0	12.0	10.0	8.0	6.0	4.0	2.0
	16,685	13,964	11,292	8,877	6,698	4,887	3,308	2,073	1,125	471	102
Network 2											
Size (m)	8.0	7.0	6.0	5.0	4.0	3.0	2.0	1.0	0.5		
	129,699	100,336	73,030	50,067	31,333	17,006	7,087	1,474	283		

Table 4 Elastic properties for the intact rock and the fractures of both study cases

	Intact rock		Fracture	
	E (GPa)	ν	K_n (GPa/m)	K_t (GPa/m)
Network 1	50.00	0.25	50.00	10.00
Network 2	84.60	0.24	434.00	86.80

Table 5 Number of successful FEM simulations for each REV size

Network 1											
Size(m)	2.0	4.0	6.0	8.0	10.0	12.0	14.0	16.0	18.0	20.0	22.0
	1000	996	996	995	990	983	976	970	962	953	950
Network 2											
Size (m)	0.5	1.0	2.0	3.0	4.0	5.0	6.0	7.0	8.0		
	994	997	987	966	935	899	839	802	751		

Table 6 Skewness and kurtosis for Network 1 data

Size	Skewness				Kurtosis			
	I1	Ex	Ey	Gxy	I1	Ex	Ey	Gxy
2 m x 2 m	0.89	0.36	0.43	-0.11	0.97	-1.06	-0.99	-0.90
4 m x 4 m	0.60	0.49	0.56	0.01	0.35	0.18	0.31	-0.21
6 m x 6 m	0.35	0.42	0.50	0.15	0.32	0.45	0.39	-0.26
8 m x 8 m	0.14	0.36	0.49	0.30	-0.08	0.11	0.39	0.14
10 m x 10 m	0.19	0.20	0.29	0.14	-0.03	-0.12	0.18	-0.10
12 m x 12 m	0.21	0.11	0.19	0.16	0.07	-0.17	0.02	0.00
14 m x 14 m	0.18	0.14	0.17	0.10	0.14	-0.09	-0.03	-0.01
16 m x 16 m	0.09	0.19	0.21	0.11	-0.01	-0.04	0.06	0.03
18 m x 18 m	0.07	0.14	0.19	0.13	-0.15	-0.15	0.01	-0.13
20 m x 20 m	0.00	0.15	0.24	0.22	-0.21	-0.24	-0.02	-0.03
22 m x 22 m	-0.07	0.21	0.29	0.21	-0.03	-0.05	0.12	0.19

Table 7 Skewness and kurtosis for Network 2 data

Size	Skewness				Kurtosis			
	I1	Ex	Ey	Gxy	I1	Ex	Ey	Gxy
0.5 m x 0.5 m	0.52	0.87	0.94	0.96	0.12	0.33	0.58	0.58
1 m x 1 m	0.25	0.80	0.64	0.77	-0.14	0.69	0.30	1.00
2 m x 2 m	0.25	0.43	0.38	0.50	-0.05	0.16	0.32	0.64
3 m x 3 m	0.18	0.24	0.31	0.28	-0.05	0.00	0.30	0.19
4 m x 4 m	0.16	0.22	0.21	0.13	-0.15	0.18	0.00	-0.06
5 m x 5 m	0.09	0.17	0.21	0.21	-0.08	0.07	0.09	0.08
6 m x 6 m	0.09	0.19	0.14	0.14	-0.08	0.09	-0.14	0.06
7 m x 7 m	0.04	0.26	0.11	0.19	0.08	0.28	0.10	0.16
8 m x 8 m	0.01	0.27	0.11	0.15	0.09	0.20	0.25	0.20

Table 8 Relative errors of the elastic properties for different REV sizes

Network 1					Network 2				
Size (m)	I_1	Ex	Ey	Gxy	Size (m)	I_1	Ex	Ey	Gxy
2	168.8%	92.5%	99.0%	72.1%	0.5	111.9%	103.0%	100.0%	81.5%
4	84.4%	46.3%	49.5%	36.0%	1	56.0%	51.5%	50.0%	40.7%
6	56.3%	30.8%	33.0%	24.0%	2	28.0%	25.8%	25.0%	20.4%
8	42.2%	23.1%	24.8%	18.0%	3	18.7%	17.2%	16.7%	13.6%
10	33.8%	18.5%	19.8%	14.4%	4	14.0%	12.9%	12.5%	10.2%
12	28.1%	15.4%	16.5%	12.0%	5	11.2%	10.3%	10.0%	8.1%
14	24.1%	13.2%	14.1%	10.3%	6	9.3%	8.6%	8.3%	6.8%
16	21.1%	11.6%	12.4%	9.0%	7	8.0%	7.4%	7.1%	5.8%
18	18.8%	10.3%	11.0%	8.0%	8	7.0%	6.4%	6.3%	5.1%
20	16.9%	9.3%	9.9%	7.2%					
22	15.3%	8.4%	9.0%	6.6%					

Table 9 Number of simulations required to obtain maximum errors of 1% and 5%

	Network 1				Network 2		
	10 m	16 m	22 m	40 m	6 m	8 m	11 m
5%	16	6	3	1	3	2	1
1%	393	153	81	25	76	43	23

Table 10 REV sizes obtained by different approaches and their maximum error for the elastic properties

	Network 1		Network 2	
	REV size (m)	Max. Error	REV size (m)	Max. Error
10 x avg. spacing	25	7.9%	5	10.5%
10 x avg. length	40	4.9%	9.2	5.7%
3 x avg. length	12	16.5%	2.8	18.7%
COV = 10%	10	19.8%	2.5	19.6%

Table 11 Confidence intervals for a sample standard deviation SD based on the chi-squared distribution with 95 % degree of confidence

Sample Size	Confidence Interval
5	0.60 SD - 2.87 SD
10	0.69 SD - 1.83 SD
50	0.84 SD - 1.25 SD
100	0.88 SD - 1.16 SD
200	0.91 SD - 1.11 SD
500	0.94 SD - 1.07 SD
1000	0.96 SD - 1.05 SD

Table 12 Average and standard deviation of the elastic moduli taken from different numbers of simulations of the reference REV size

	Simulations	Average (GPa)			Standard deviation (GPa)		
		Ex	Ey	Gxy	Ex	Ey	Gxy
Network 1	996	26.43	25.04	12.85	4.16	4.21	1.57
	50	26.07	24.84	12.67	4.01	4.27	1.59
	10	26.36	24.60	12.77	4.30	4.34	1.62
Network 2	966	27.22	25.54	9.97	2.31	2.13	0.89
	50	27.44	25.62	10.04	2.21	2.05	0.96
	10	27.22	25.30	9.91	2.22	1.97	0.80

Table 13 Relative errors associated to the selected samples of 50 and 10 REVs of the reference sizes

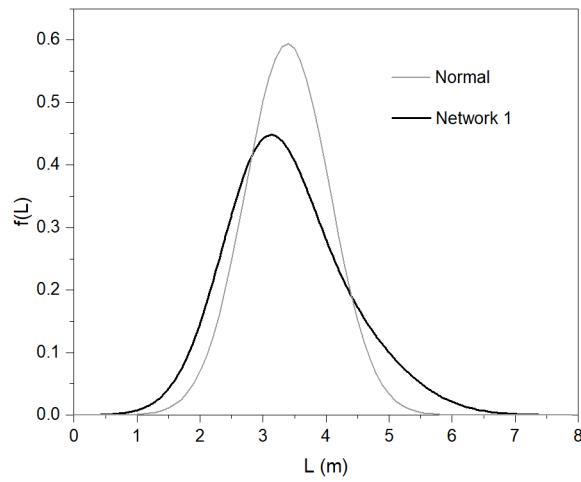
	Simulations	t*	Network 1 (22 m)			Network 2 (8 m)		
			Ex	Ey	Gxy	Ex	Ey	Gxy
Network 1	Maximum	1.96	8.4%	9.0%	6.6%	6.3%	6.1%	6.6%
	50	2.01	8.4%	9.4%	6.9%	6.1%	6.1%	7.2%
	10	2.26	10.1%	10.9%	7.8%	6.9%	6.6%	6.8%

Table 14 Data for the Uniaxial Compressive Strength in Esmaili et al (2010)

REV size	Number of samples	Av. number of fractures	Std. Dev. UCS (MPa)
1.5 m x 1.5 m x 3.0 m	5	30.8	42.7
3.5 m x 3.5 m x 7.0 m	5	197.1	17.8
7.0 m x 7.0 m x 14.0 m	5	1214.4	8.9
10.0 m x 10.0 m x 20.0 m	5	152.1	3.6

Table 15 Data for the Uniaxial Compressive Strength in Farahmand et al (2017). The data was retrieved from Fig.14 of the paper.

REV size	Number of samples UCS	Std. Dev. UCS (MPa)
5.0 m x 2.0 m	8	25.6
7.0 m x 2.8 m	7	9.2
8.0 m x 3.2 m	5	6.9
9.0 m x 3.6 m	4	4.6
10.0 m x 4.0 m	3	3.7

**Fig. 1** Resulting probability distribution function for the fracture length of Network 1, according to the data in (Yang et al., 2014)

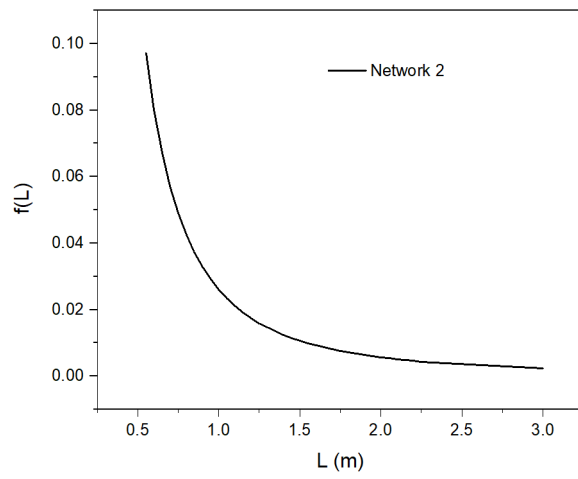


Fig. 2 Probability distribution function for the fracture length of Network 2, according to the data in (Min and Jing, 2003)

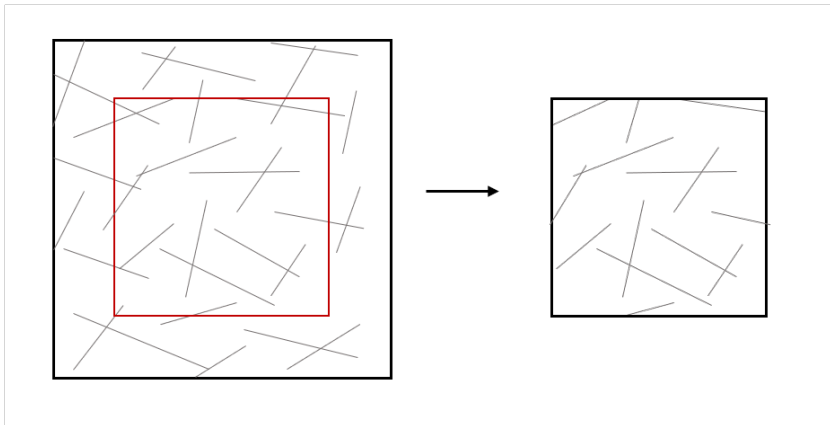


Fig. 3 Generation of smaller REVs from bigger ones: geometrical center is maintained, external fractures are removed and boundary intersections are adjusted

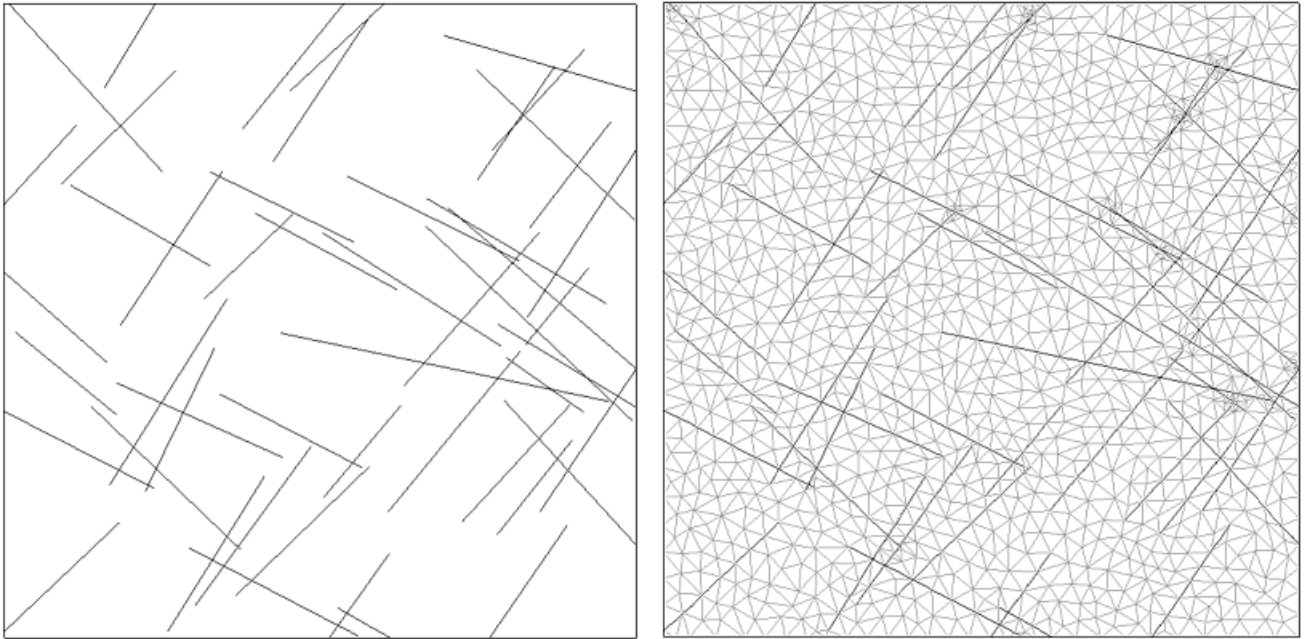


Fig. 4 Example of a DFN and associated mesh in a 10 m x 10 m REV for Network 1

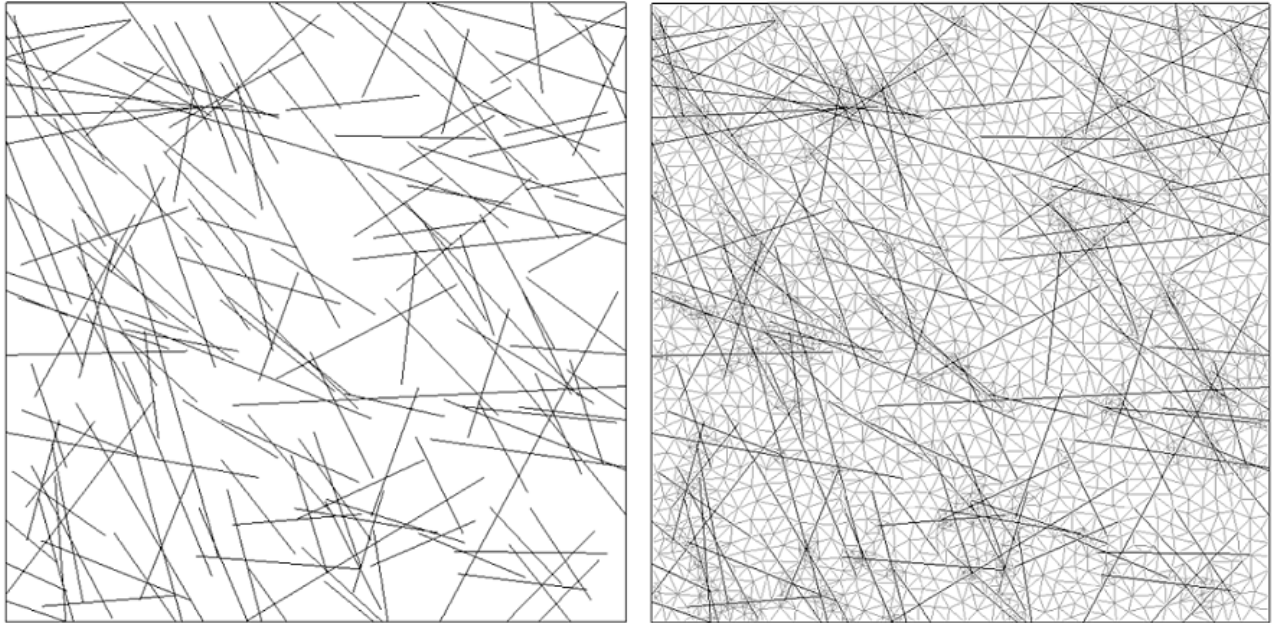


Fig. 5 Example of a DFN and associated mesh in a 3 m x 3 m REV for Network 2

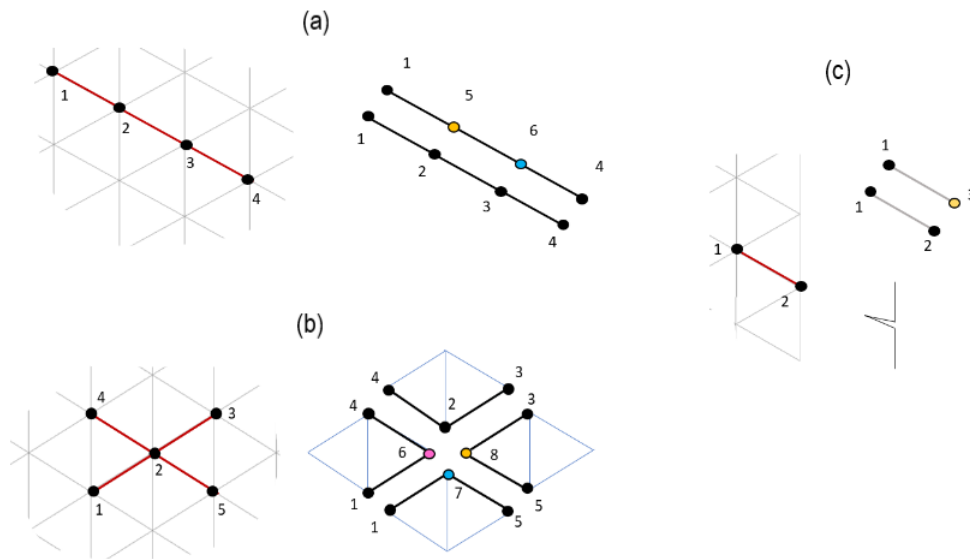


Fig. 6 Creation of interface elements and change of connectivity for surrounding bulk elements in three possible scenarios: a) one fracture b) several intercepting fractures c) fracture and at the boundary of the domain

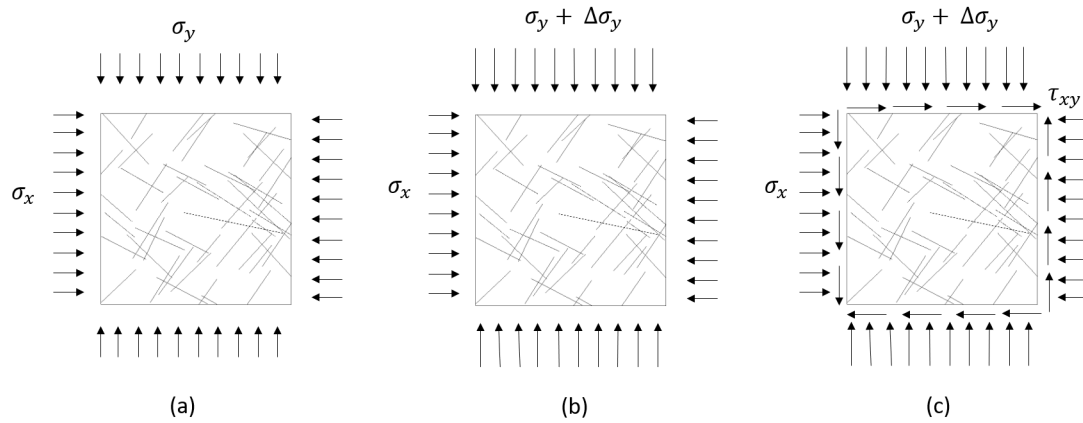


Fig. 7 Three linearly independent stress boundary conditions are applied in three steps: a) initial biaxial conditions b) stress in y direction is increased c) application of shear stress

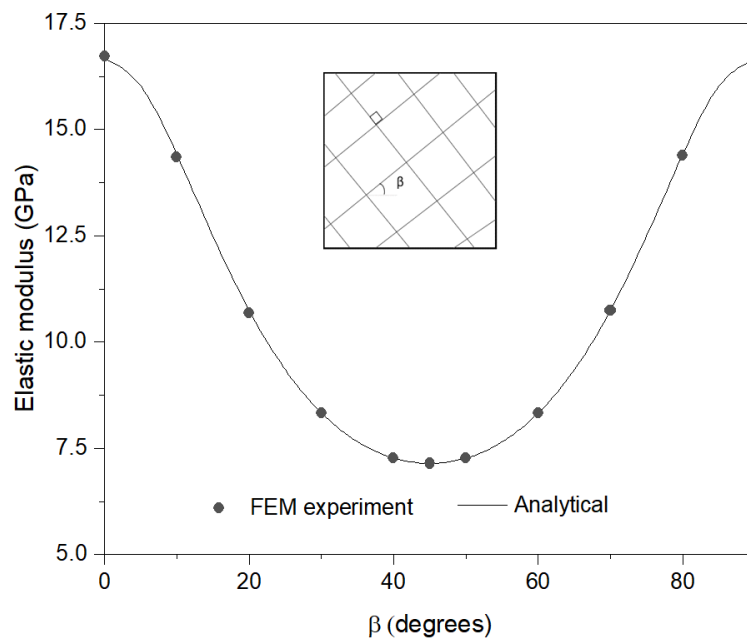


Fig. 8 Validation of the finite element code: comparison with the analytical solution of the equivalent modulus of an REV containing two perpendicular sets of persistent fractures for different orientations β .

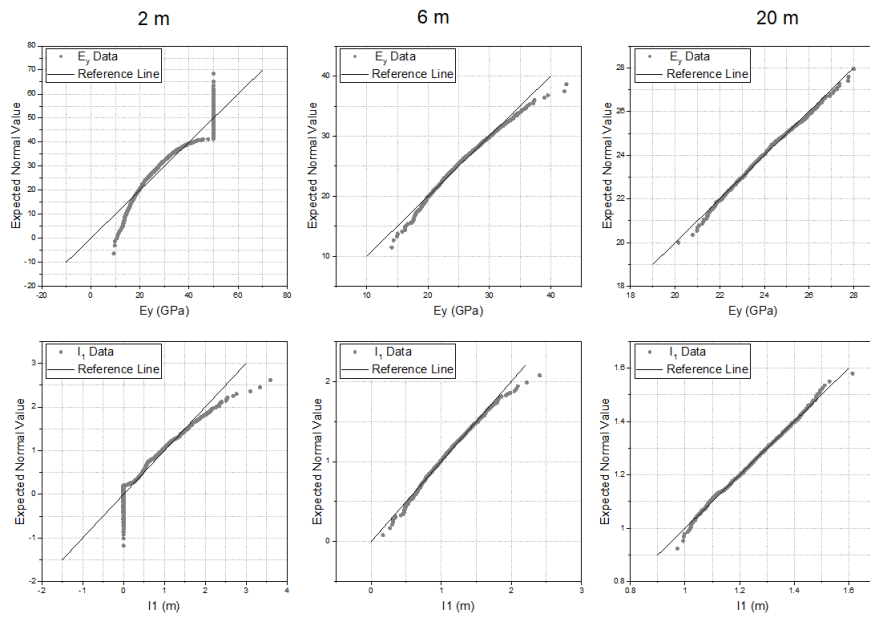


Fig. 9 Q-Q plot for the elastic modulus (upper graphs) and first invariant of the fracture tensor (lower graphs) - Network 1

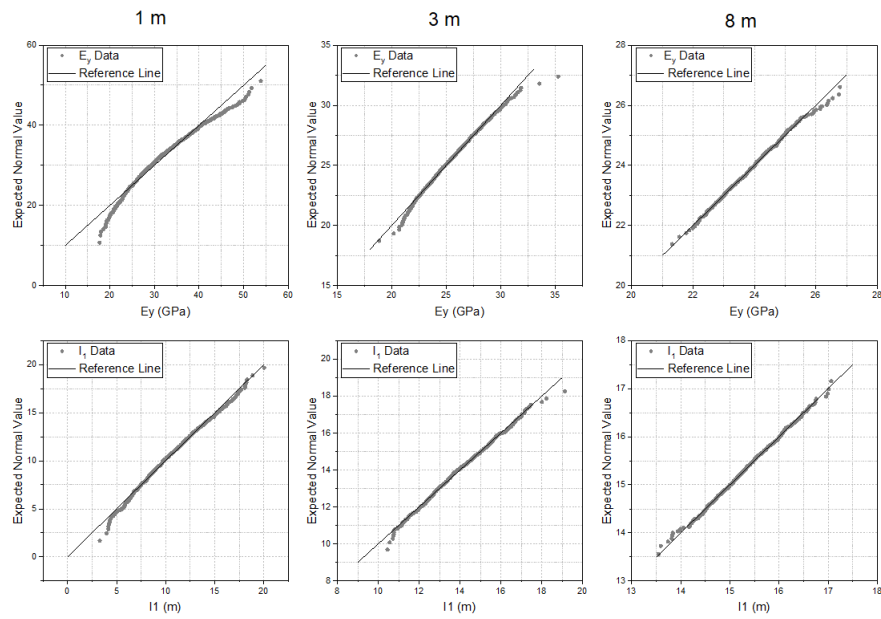


Fig. 10 Q-Q plot for the elastic modulus (upper graphs) and first invariant of the fracture tensor (lower graphs) - Network 2

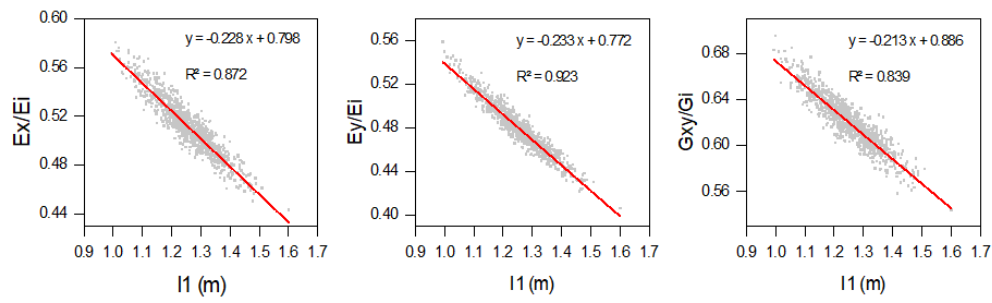


Fig. 11 Equivalent elastic moduli normalized by the elastic moduli of the intact rock, E_i and G_i , vs first invariant - Network 1

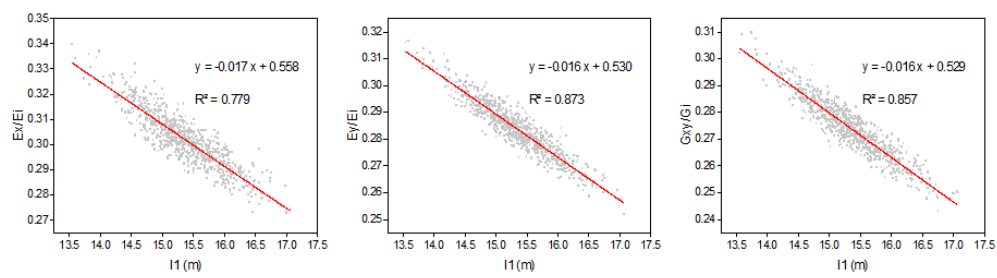


Fig. 12 Equivalent elastic moduli normalized by the elastic moduli of the intact rock, E_i and G_i , vs first invariant - Network 2

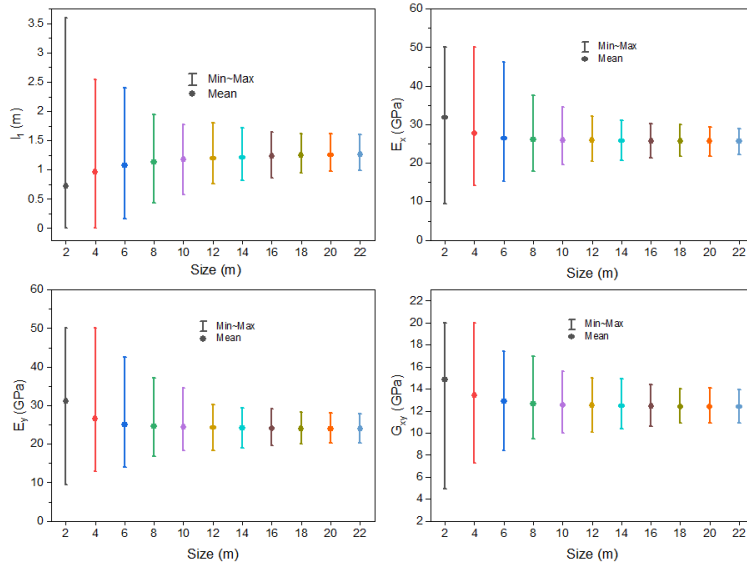


Fig. 13 Average, minimum and maximum moduli for Network 1

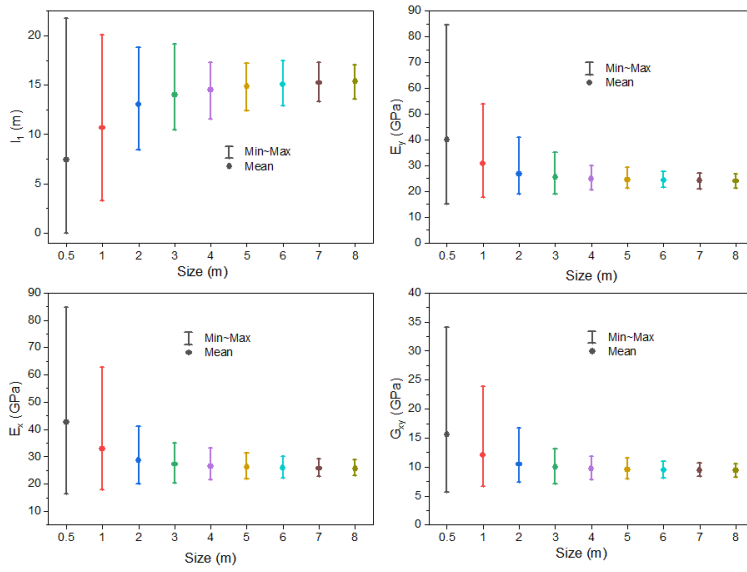


Fig. 14 Average, minimum and maximum moduli for Network 2

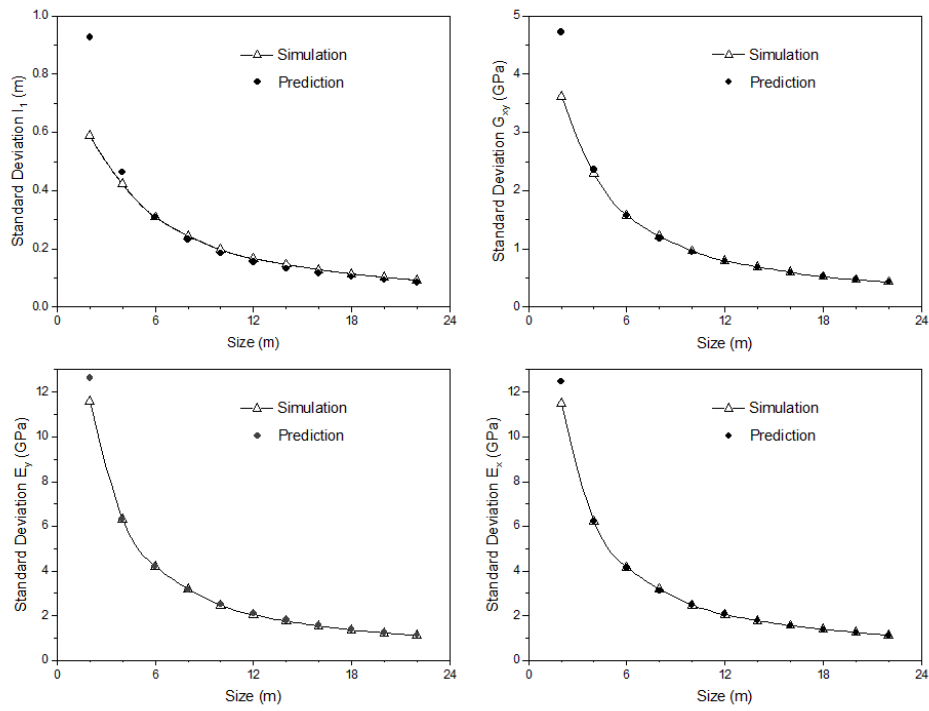


Fig. 15 Comparison of standard deviations of the simulated samples with those predicted from the reference volume of 6 m - Network 1

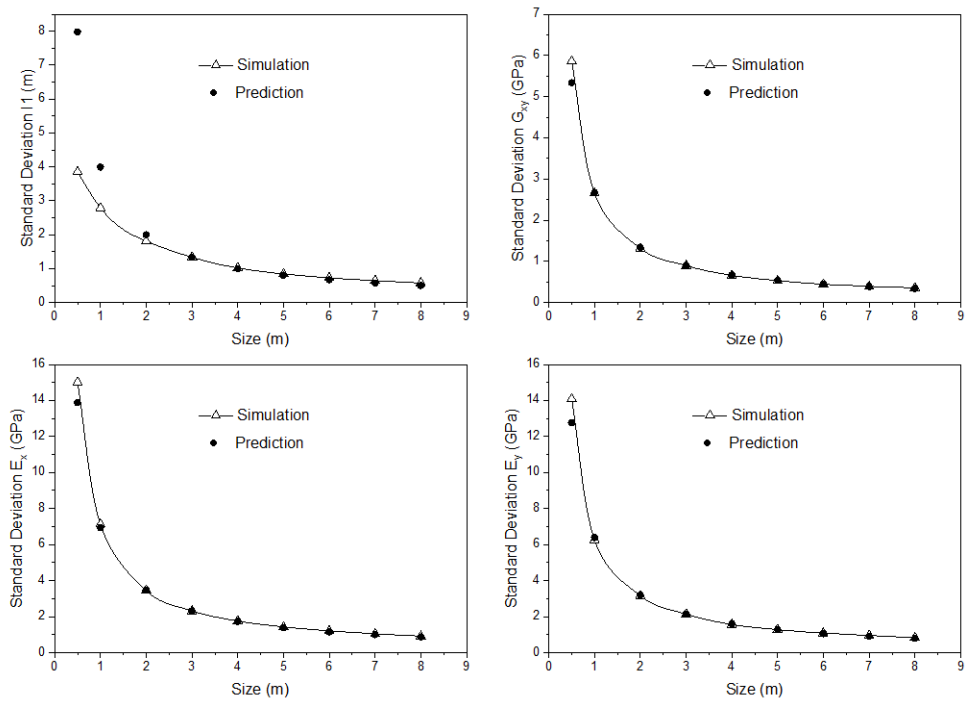


Fig. 16 Comparison of standard deviations of the simulated samples with those predicted from the reference volume of 3 m - Network 2

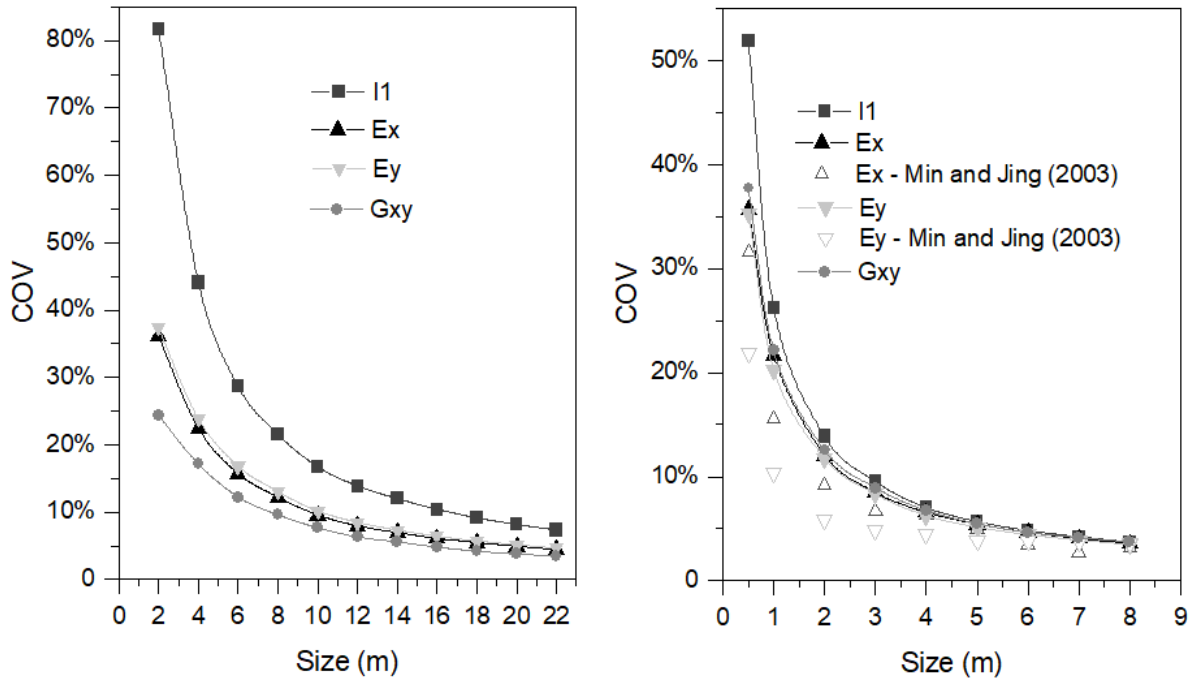


Fig. 17 Coefficients of variation (COV) of the first invariant of the fracture tensor and the elastic moduli for Network 1 (left) and Network 2 (right)

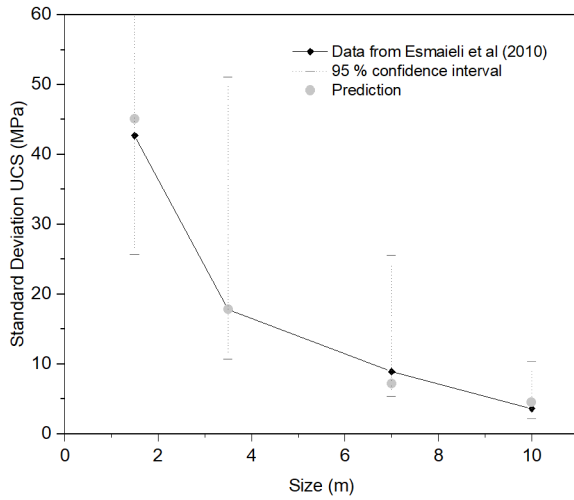


Fig. 18 Standard deviations of the UCS obtained by Esmieli et al (2010) and those predicted with Equation 12 from the reference volume with side 3.5 m

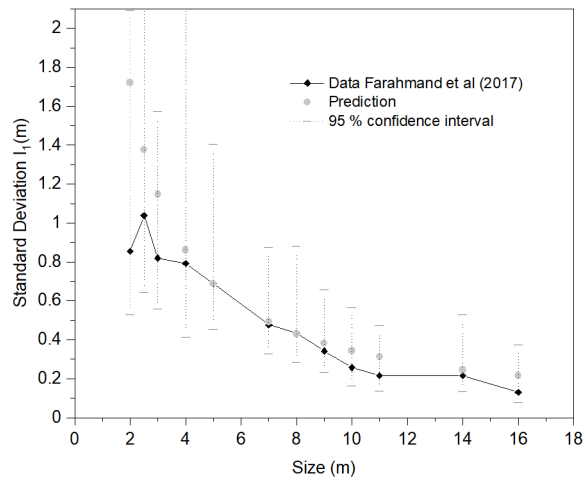


Fig. 19 Standard deviations of the first invariant of the fracture tensor obtained by Farahmand et al (2017) and those predicted with Equation 13 from the reference volume with side 5 m

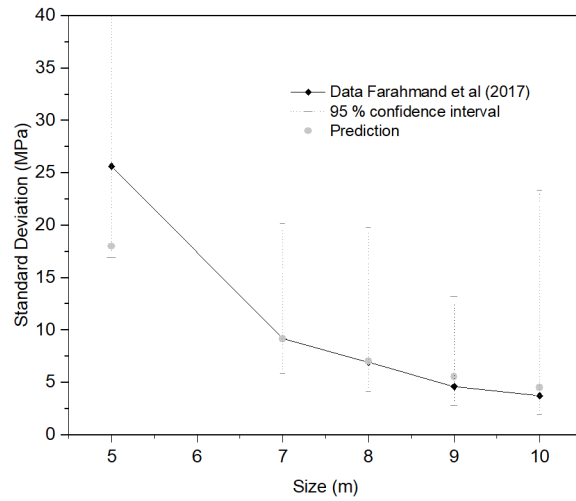


Fig. 20 Standard deviations of the UCS obtained by Farahmand et al (2017) and those predicted with Equation 13 from the reference volume with side 7 m